

# Constraining Sterile Neutrinos with pGRAMS: A Sensitivity Study for Supernova Gamma Rays

Report for Summer 2025 REU Program at Columbia University - Nevis Labs

Ayden Gertiser\*

University of Texas at Austin, Department of Physics, Austin, TX

(Dated: August 1st, 2025)

GRAMS (Gamma-Ray and AntiMatter Survey) has the potential to provide bounds on the parameter space for sterile neutrinos produced in core-collapse supernovae. To explore this possibility, a sensitivity study for its predecessor, pGRAMS, is performed. This report details the motivation for such an experiment, necessary background modeling for the (p)GRAMS balloon experiment, and describes the sensitivity estimates in mass/mixing angle parameter space. We report a preliminary  $2\sigma$  ability to measure  $\log |U_{\tau 4}|^2 = -14.1$  for 200 MeV sterile neutrinos and  $\log |U_{\tau 4}|^2 = -11.1$  for 50 MeV sterile neutrinos.

## I. INTRODUCTION

### A. GRAMS and Its Motivation

Gamma-ray astronomy is crucial to studying high-energy astrophysical processes such as supernovae, pulsars, active galactic nuclei, and potential dark matter decay or annihilation. High-energy photons travel largely unimpeded through the cosmos, making them ideal messengers of distant or obscured phenomena. While keV and GeV/TeV gamma rays have been extensively observed by instruments such as NuSTAR and Fermi, respectively, the MeV range (approximately 0.1–100 MeV) remains relatively unexplored (Figure 1). This so-called "MeV Gap" in observations is due to several factors including large atmospheric background from cosmic rays, difficulty of Compton reconstruction, and strong nuclear gamma-ray background generated by the detector itself[1, 2].

GRAMS (Gamma-Ray and AntiMatter Survey) is a proposed long-duration balloon flight (LDB) and ultimately satellite mission aimed at bridging the MeV sensitivity gap using a liquid argon time projection chamber (LArTPC) as a Compton camera, while the antimatter survey aims to detect anti-deuteron excess arising from dark matter annihilation. In preparation, a precursor experiment, pGRAMS, has been proposed and is scheduled for a short test flight in 2026. If successful, a future, longer ( $\sim 30$  days) flight is envisioned for pGRAMS over with Sweden or New Zealand as a science mission, as early as 2028, followed by the first GRAMS science balloon flight.

The pGRAMS detector will contain an active volume of liquid argon of dimensions  $30 \times 30 \times 20$  cm, and is surrounded by two layers of plastic scintillators that

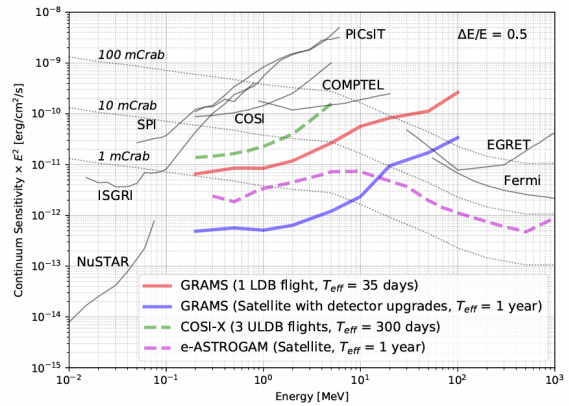


Figure 1. The continuum gamma-ray sensitivities at a  $3\sigma$  confidence level of current and future experiments, demonstrating the lack of instruments with high-sensitivity in the MeV range [1].

function as time-of-flight detectors for charged particles. In the gamma-ray survey, the plastic scintillators are used to veto charged particles. The active volume is also separated into 9 optically-isolated cells using polytetrafluoroethylene (PTFE, or Teflon). These barriers are opaque to scintillation photons to assist in position reconstruction, but are transparent to gamma rays by virtue of their extraordinarily small wavelength.

To determine the MeV gamma-ray source location and energy, the LArTPC functions as a Compton camera and calorimeter (Figure 2). Silicon photomultipliers (SiPMs) are positioned at the bottom, which when combined with ionization detectors at the top provide three-dimensional position reconstruction of charged-particle tracks and Compton scatters. Once the Compton scatters are located, the Compton equation can be used to determine the energy of the primary gamma ray. Calculations of reconstructed energies can be found in Appendix A.

\* Correspondence email address: ayden.gertiser@utexas.edu

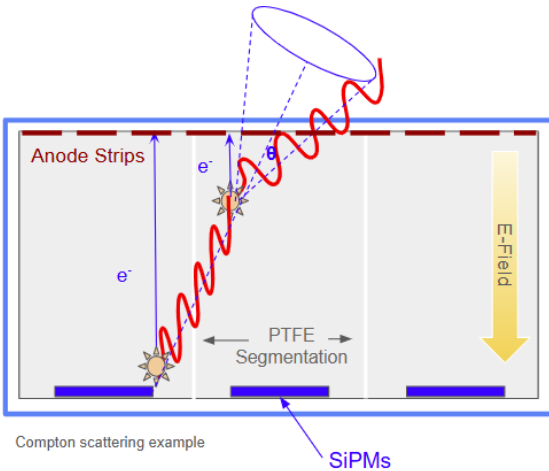


Figure 2. GRAMS detection concept [1].

## B. Sterile Neutrinos

To date, experimentalists have confirmed the existence of three active neutrino flavors: the electron neutrino, muon neutrino, and tau neutrino, each associated with its corresponding charged lepton. These neutrinos are electrically neutral and interact only via the weak force and gravity. They are arguably the most elusive of the known particles, and their discovery in the 20th century highlights the extraordinary predictive power of the Standard Model. However, over the past seventy-five years, it has become more and more clear that the particles and interactions of the Standard Model are insufficient to describe many astrophysical observations. Measurements of the cosmic microwave background from the Wilkinson Microwave Anisotropy Probe (WMAP) indicate that dark matter contributes roughly five times more to the universe's energy density than ordinary matter, none of which is explained by Standard Model particles[3]. One well-motivated candidate is the *sterile neutrino*, a hypothetical right-handed neutrino which like the active neutrinos does not participate in electromagnetic or strong interactions, but unlike the active neutrinos, do not interact with the weak force. Despite the sterile neutrino's gauge-singlet nature, it could still play a crucial role in cosmology by contributing to structure formation and dark matter density through gravitational interactions.

Interestingly, despite the seemingly inert nature of the sterile neutrino, mechanisms exist that would allow for its indirect detection. Evidence for neutrino oscillations, as observed in experiments such as Super-Kamiokande and SNO shows that neutrinos can transform between flavors[4]. This discovery also leads us to the conclusion that neutrinos must have mass. To see this, consider a massless neutrino. From a relativistic

standpoint, the neutrino would propagate at the speed of light and therefore be unable to undergo unitary time evolution. This would have eliminated the possibility of flavor oscillations.

The discovery of massive neutrinos (yet  $<0.8$  eV)[5] opens the door to theoretical mechanisms that would explain the very small masses of the active neutrinos. One such framework is the seesaw mechanism, which involves the heavy right-handed sterile neutrinos. In this model, the large mass of the sterile neutrinos suppresses the masses of the active neutrinos. However, the large mass and singlet nature of sterile neutrinos make them extraordinarily difficult to detect directly. Searches must rely on indirect detection techniques, such as observing potential decay signatures in the gamma-ray sky[6], which is possible with GRAMS.

## C. GRAMS Simulation Software

GramsSim is an end-to-end simulation software framework for the (p)GRAMS detector developed by GRAMS Collaborators[7]. It has several components, including generation of primary particles (GramsSky), modeling of interactions in liquid argon (GramsG4), and others documented on the GramsSim Github page.

**GramsSky:** The function of GramsSky is to create the primary particles that will interact with the detector. The particle generation process is very similar to that of the Geant4 General Particle Source (GPS)[8]. Most importantly for this work, it allows for point source generation primary particles or with energy and position sampled from histograms and HEALPix maps. The primary difference between particle generation using GramsSky vs. Geant4 GPS is that in GramsSky, after a particle on the surrounding sphere is generated, it is translated randomly on a disk tangent to the sphere at this point (Figure 3)[7]. The purpose of this is to simulate the effect of particles being generated from a very distance source.

**GRAMSG4:** GramsG4 is how GramsSim simulates the movements of particles through matter, and in order to do so is built off of Geant4[8]. GramsSky can be (and was in this analysis) used to generate the particle input to GramsG4, however, this can alternatively be done using Geant4 macro files. Upon running GramsG4, a ROOT file is generated containing information about each event (primary particle) including the event ID (EventID), which includes metadata on each particle, (TracksList), and the deposited energy for the liquid argon and surrounding scintillators (LArHits, ScintHits). All simulations are run using the FTFP\_BERT\_LIV+OPTICAL+STEPLIMIT[8] physics lists.

The remainder of this report is organized as follows. Section 2 introduces the sterile neutrino model and ex-

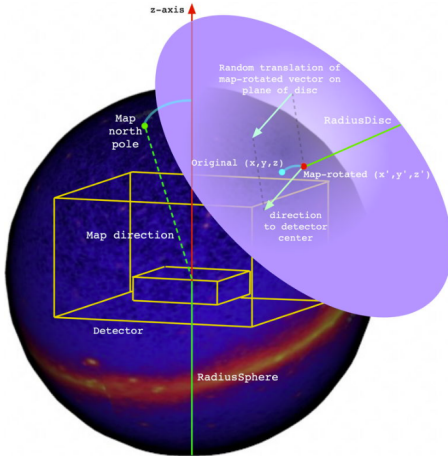


Figure 3. Process of GramsSky particle translation to simulate particle being produced at "infinity".

pected supernova flux. Section 3 details the gamma-ray backgrounds relevant to balloon-borne detectors. Section 4 describes the simulation and event selection process and the statistical sensitivity analysis, and section 5 concludes with next steps and future improvements.

## II. STERILE NEUTRINO FLUX

One way that heavy sterile neutrinos can be produced is in core-collapse supernovae. Due to the enormous neutron density in the cores of stars, this would proceed most commonly as a neutrino-neutron scattering process ( $\nu_l + n \leftrightarrow n + N$ ), but sterile neutrinos can also be produced by interactions with electrons, positrons, muons, protons, and (anti)neutrinos. Once a sterile neutrino is produced, it propagates outwards before eventually decaying, emitting decay products isotropically in the sterile neutrino rest frame (Figure 4). There are a few possibilities for the decay products, but only a couple would create a potential gamma-ray signature. The first is the  $N \rightarrow \gamma + \nu$ . For  $N$  masses below the pion mass threshold (135 MeV), this is the only decay process that leads to photon production. Above the pion mass threshold, the decay  $N \rightarrow \pi^0 + \nu$  becomes possible, with the  $\pi^0$  decaying nearly instantly ( $\sim 85$  attoseconds) into two gamma rays. For a supernova occurring 10 kpc away from Earth, flux maps differential in time and energy can be generated following the methods of [6](Figure 5). Notably, because neutrinos travel almost entirely unhindered by the star, the gamma-ray flux from sterile neutrino decay occurs long before the rapid expulsion of photons most commonly associated with supernovae, and thus escape the very large background flux that follows.

It should also be noted that a purely right-handed

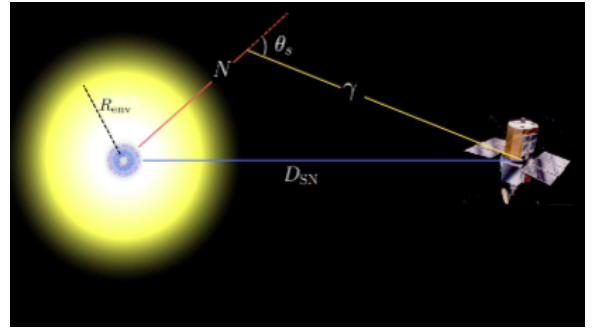


Figure 4. Sterile neutrino decay geometry [6]

sterile neutrino is invisible to the weak force. Neutrino oscillations tell us that the mass eigenstates and the flavor eigenstates of neutrinos are distinct. For the active neutrinos, the relation is described by the PMNS matrix:

$$\nu_\alpha = \sum_i U_{\alpha i}^* \nu_i$$

where  $\alpha = e, \mu, \tau$  are the labels of the flavor eigenstates and  $i = 1, 2, 3$  are the labels of the mass eigenstates. The introduction of sterile neutrinos raises the question of how they mix with the active neutrinos. In particular, if the sterile neutrino can mix with the active neutrinos, then it could experience a suppressed weak force interaction, allowing for decay into detectable signatures. Matrix elements for the decay rates are calculated [6] for these decays as a function of squared mixing angle ( $|U_{\alpha 4}|^2$ ):

$$N \rightarrow \nu_\alpha + \gamma : \Gamma = \frac{9\alpha M_N^5}{2048\pi^4} G_F^2 |U_{\alpha 4}|^2$$

$$N \rightarrow \nu_\alpha + \pi^0 : \Gamma = f_\pi^2 \left(1 - \frac{m_{\pi^0}^2}{M_N^2}\right) \cdot \frac{G_F^2 |U_{\alpha 4}|^2 M_N^3}{32\pi}$$

where  $\alpha \approx 1/137$  is the fine structure constant,  $G_F = 1.166 \cdot 10^{-5} / \text{GeV}^2$  is the Fermi constant, and  $f_\pi = 135$  MeV is the pion decay constant.

Aside from the raw flux from sterile neutrino decay, a balloon experiment must also consider the attenuation of gamma rays by the atmosphere. By definition, the transmittance  $T$  is defined by  $T = e^{-\tau}$ , where  $\tau$  is the optical depth. From the Beer-Lambert law, we have that for attenuation cross section  $\sigma_i$  and density  $n(z)$ ,

$$\tau = \sum_i \tau_i = \sum_i \sigma_i \int_a^b n_i(z) dz$$

For a balloon experiment operating at 30,000 meters above sea level, we can integrate the density from  $h =$

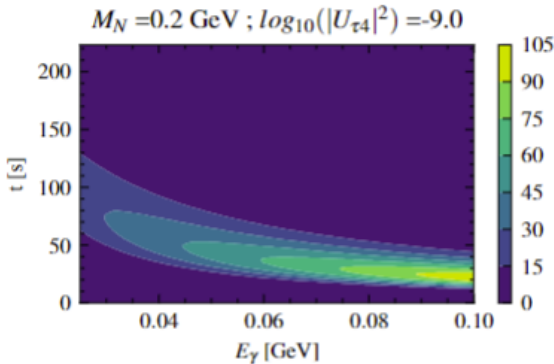


Figure 5. Example double-differential flux map for gamma rays produced in sterile neutrino decay from a supernova at a distance of 10 kpc in units of  $\text{ph}/\text{cm}^2/\text{s}/\text{GeV}$ . This does not take into account atmospheric attenuation.  $t = 0$  is the time of the first neutrino signal on Earth. [6]

$\infty$  to  $h = 30,000$  m using atmospheric densities tabulated by NASA [9], arriving at a value of  $11.9 \text{ g/cm}^2$ . The attenuation cross sections are tabulated in the NIST XCOM database. For an atmospheric mixture of 80% nitrogen and 20% oxygen, they report a near-constant  $1.6 \cdot 10^{-2} \text{ cm}^2/\text{g}$  in the  $30 - 100$  MeV range. Together, these give a transmission value of

$$T = e^{-11.9 \cdot 0.016} = 83\%$$

To account for this, all gamma ray fluxes from sterile neutrinos are multiplied by 0.83 when performing sensitivity calculations. Note that this is already accounted for in the cosmic ray flux calculated by EXPACS (see next Section).

### III. SIMULATION OF BACKGROUNDS

In any sensitivity study, it is paramount to model background noise as accurately as possible. For a balloon experiment like pGRAMS, the main backgrounds are atmospheric backgrounds from cosmic ray interactions in air, with small contribution from the cosmic diffuse gamma-ray emission.

#### A. Atmospheric Backgrounds

By far the most prevalent background for an MeV balloon experiment is from secondary particles arising from atmospheric cosmic ray interactions (Figure 6). Among these are gamma rays, neutrons, and a large variety of charged particles. Photons are the most common among these in this energy range, so these are the only output considered in the background modeling. There

is, of course, still a significant flux coming from neutrons and charged particles. However, the pGRAMS plastic scintillator will be capable of vetoing charged particles, and neutrons can be vetoed by looking at the ratio of scintillation light to ionization charge as is done in many liquid noble experiments [10].

The software "EXcel-based Program for calculating Atmospheric Cosmic-ray Spectrum" (EXPACS) [11] has been developed for modeling these backgrounds. EXPACS considers protons and heavy ions as primary particles. Flux maps of these secondary particles can be generated in HEALPix maps, which can then be input to GramsSky for primary particle generation.

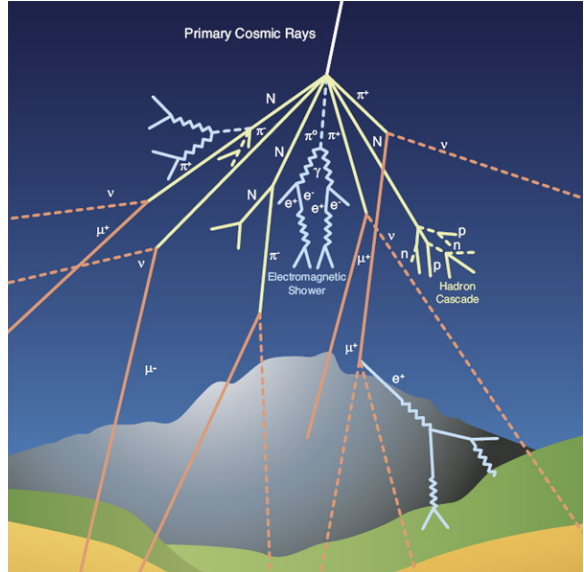


Figure 6. Atmospheric cosmic ray shower. Source: CERN

As of writing, EXPACS only has cosmic ray flux data up to February 28th, 2025, and as such this most recent data was used for atmospheric background model. This is easy to update once data is released for the time of the experiment. Cosmic ray flux is also highly dependent on the location on Earth. The pGRAMS science flight is set to fly over either Sweden or New Zealand; the Sweden location at the Esrange Space Center in Kiruna ( $67.9^\circ \text{ N}, 21.1^\circ \text{ E}$ ) was used for this analysis.

#### B. Cosmic Emission

A weaker source of gamma ray background are the gamma rays coming from the galactic plane. These gamma rays come primarily from cosmic ray interactions in the interstellar medium, along with various sources like blazars and active galactic nuclei (AGNs), which generate gamma rays via inverse Compton scattering and other mechanisms.

Much of the MeV-sky background has already been documented and collected in FITS files on the "MeV All Sky" site<sup>1</sup>. These maps include a catalog of sources, the galactic diffuse emission, and the extragalactic diffuse emission. These maps are in galactic coordinates, so to implement them into a balloon simulation we must transform them into detector coordinates. This transformation is done using the Python package Astropy [12]<sup>2</sup>. This flux map transformation does not take into account the Earth itself, which will block flux coming from behind the Earth toward the instrument (Figure 7). This cutoff point is calculated separately by the method documented in Appendix B.

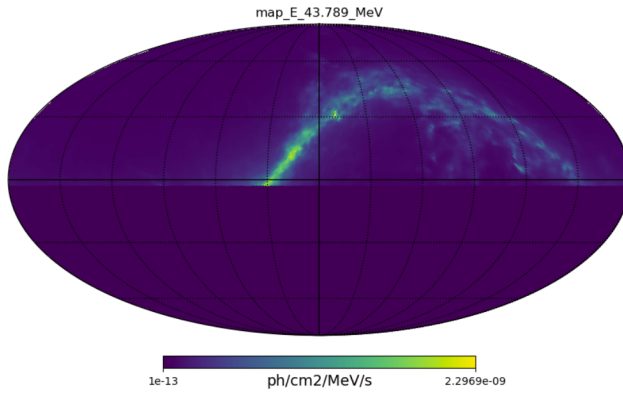


Figure 7. 43.789 MeV flux map of the cosmic gamma-ray emission transformed from galactic coordinates to Alt-Az observer coordinates (Esrang Space Center, April 1st, 2026, 8 PM local time, 30 km above ground). The map below the horizon line is set to very low flux to avoid sampling in this region.

The magnitude of the total flux in the region of interest (30 - 100 MeV for sterile neutrino decay), the cosmic diffuse emission is less than 0.1% of the atmospheric emission, and is thus mostly ignored in a pGRAMS analysis. However, for a satellite experiment like GRAMS, it becomes much more important because of the lack of atmosphere that would facilitate cosmic ray showers.

### C. Signal and Background Event Selection

An array of selection cuts are made when simulating backgrounds and signal that reflect the predicted ability of pGRAMS to make such cuts. The first of these is to consider only primary gamma rays that undergo at

least three interactions in the detector—for example, a photon that undergoes two Compton scatters and then a photo-absorption, or greater than two Compton scatters. We also assume that we will be able to veto all events from charged particles using the plastic scintillator system, and veto nuclear recoils using the pulse shape analysis techniques that have been developed in various liquid-noble TPCs like LUX [10]. Reconstruction of event energies and sky location in the 30-100 MeV range can be very difficult using Compton scattering as a result of pair production and bremsstrahlung dominating in this energy range (Figure 8). Additionally, we find that for events with 2 Compton scatters and a third interaction, these vertices tend to be very close together at high energies, which if we require the successive scatters to be in unique optically isolated cells, this drastically drops selection efficiency. This highly motivates the development of better reconstruction algorithms to handle high energy Compton events, and approaches that can select pair production with high efficiency and good energy and angular resolution.

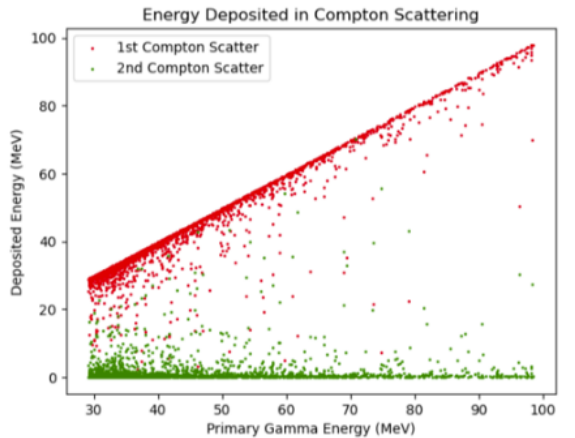


Figure 8. Energies of Compton scattered electrons. Electrons ejected in the first scatter have more than enough energy to create high-energy bremsstrahlung photons.

### IV. SENSITIVITY

To evaluate the detector sensitivity to a supernova signal, we first define the source location on the sky. In this analysis, we assume the supernova occurs directly overhead the detector, and we accept only events within a 2° cone centered at zenith. This angular cut is motivated by three factors: (1) the atmospheric background flux is lowest near zenith due to the reduced air column; (2) the available background simulation data becomes sparse and unreliable below this angle, leading to nu-

<sup>1</sup> <https://tsuji703.github.io/MeV-All-Sky/>

<sup>2</sup> [github.com/Gertibird/GRAMSNevisREU2025](https://github.com/Gertibird/GRAMSNevisREU2025)

merical instability; (3) larger angular windows would dilute the signal-to-background ratio. To implement this cut in the simulation, we modify the EXPACS flux map to mask all directions outside the  $2^\circ$  cone. This masked map is then used as input to GramsSky. Although the pGRAMS detector's intrinsic angular resolution is finer than  $2^\circ$ , this wider cone ensures adequate statistics and suppresses background, while accounting for potential balloon drift over the 3600 second time interval being considered, with  $t = 0$  corresponding to the initial neutrino detection.

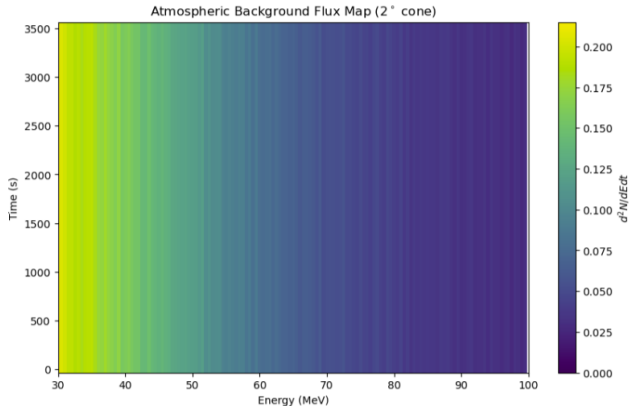


Figure 9. Double Differential flux for atmospheric background.

The next important step is to incorporate the time-dependent nature of the gamma-ray flux from decaying sterile neutrinos. GramsSky does not inherently handle time dependence, so an approximation was used. Individual GramsSim files for each time bin were generated and separately analyzed over the simulated background counts. Supernova flux data is taken over 3600 seconds in 50 time bins, making for 72 seconds per file. While this binning is much more coarse than the expected temporal resolution of the pGRAMS detector, it balances fidelity with computational feasibility. Generating higher-resolution time bins would require hundreds or thousands of simulation files, which is prohibitive under computational and time constraints during this REU project.

The pGRAMS' significance level is calculated as follows. (1) Using GramsSky and GramsG4, simulate 100,000 background events per time bin and 1,000 events per time bin of sterile neutrino signal events. The signal events are sampled from histograms acquired by the energy-time differential flux map. Run these events through the cuts described to arrive at a simulated counts distribution. (2) Determine the physical flux in the energy range being considered. For the atmospheric background, we calculate a flux of  $.00015 \text{ ph/cm}^2/\text{s}$ . The signal flux varies largely over the 3600 seconds.

(3) Calculate the number of physical photons expected. pGRAMS has dimensions of  $30 \times 30 \times 20 \text{ cm}$ , so the total number of photons from the atmosphere is  $.00015 \times 30^2 \times 72 = 9.72$  photons per 72 seconds. (4) Adjust the simulated counts distribution to reflect the correct number of physical photons. This requires multiplication by the number of expected photons divided by the number of simulated primary photons. This also includes multiplying the signal by .83 to reflect atmospheric attenuation. (5) Now that each time and energy bin has the correctly normalized number of counts, run a likelihood test between the background only distribution and the signal+background distribution ( $n$  is the expected count,  $v$  is the observed counts).

$$\ln \lambda = - \sum_i \left( n_i \ln \frac{n_i}{v_i} + v_i - n_i \right)$$

(6) Because there are low counts in each time bin, we cannot assume that a  $\chi^2$  approximation works here. Instead, we simulate Poisson noise over the background distribution, and determine the significance level by counting the number of toy experiments with test statistic greater than the observed (signal plus background) test statistic.

Our results (Figure 10) demonstrate that for  $M_N = 200$  and  $M_N = 50$ , MeV, we estimate a  $2\sigma$  sensitivity to  $|U_{\tau 4}|^2 = -15.1$  and  $|U_{\tau 4}|^2 = -12.1$  respectively if we are able to reconstruct 100% of out energies, which could be rather optimistic. On the pessimistic end, if we are only able to reconstruct .1% of our 30-100 MeV events, pGRAMS is would have  $2\sigma$  sensitivity to  $|U_{\tau 4}|^2 = -14.1$  ( $M_N = 200$  MeV) and  $|U_{\tau 4}|^2 = -11.1$  ( $M_N = 50$  MeV)

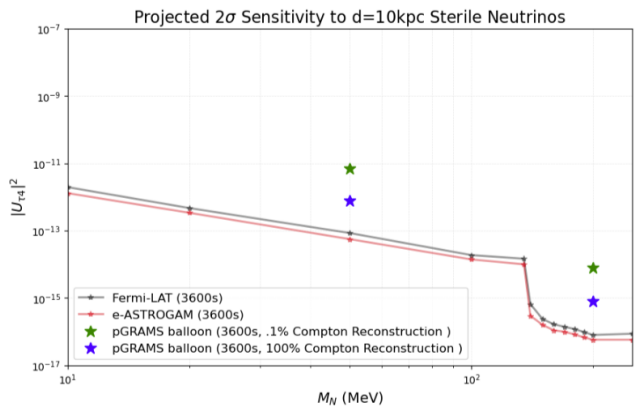


Figure 10. Estimated  $2\sigma$  sensitivity of pGRAMS to sterile neutrinos from a  $d=10$  kpc supernova occurring directly above the detector.

## V. CONCLUSION

To summarize, the (p)GRAMS LAr TPC technology allows for reconstruction of energy and position of astrophysical signals from MeV gamma ray sources. Using detector simulations, we've created a workflow to study the sensitivity of (p)GRAMS to these cosmic signals. In the case of sterile neutrino decay, we have demonstrated initial capabilities of pGRAMS to limit mass/mixing angle parameter space, suggesting optimism for the GRAMS detector and future MeV gamma-ray experiments.

Naturally, there are improvements that can be made to this analysis. The most obvious one is that this analysis was not run on the official pGRAMS detector geometry. As of the submission of this paper, the GDML (geometry file used to simulate realistic detector volume/properties) file is still in progress. Afterwards, a very similar analysis can be carried out on the full GRAMS detector geometry. Next, occupancy studies need to be done to determine how well we are able to distinguish individual events. This analysis assumes

that we are able to do so. As mentioned earlier, further study of pGRAMS ability to reconstruct high energy events is paramount to determining the effective area in this energy range. Finally, it will be important to include errors introduced by particles other than gamma rays. This analysis assumes that the plastic scintillator and pulse shape analysis will be enough to make this effect insignificant, but more thorough study is required.

## ACKNOWLEDGEMENTS

I would like to thank Prof. Georgia Karagiorgi, Prof. Reshma Mukherjee, Dr. Jon Sensenig, Dr. William Seligman, Svanik Tandon, and Dr. Naomi Tsuji for their incredible guidance and support. I would also like to thank Amy Garwood and the rest of the administration at Nevis Labs for being incredibly helpful in making this summer as productive and enjoyable as possible. If in the future I work with people even half as wonderful, I would consider myself very lucky. This material is based upon work supported by the National Science Foundation under Grant No. PHY-2349438.

---

[1] T. Aramaki, P.H. Adriana, Georgia Karagiorgi, Hiroyaku Odaka, *Dual MeV Gamma-Ray and Dark Matter Observatory - GRAMS Project* (arXiv:1901.03430v3 5 Dec 2019).

[2] A. Zoglauer et al., *Gamma-ray Astrophysics in the MeV Range, The ASTROGAM Concept and Beyond* (arXiv:2102.02460v1 4 Feb 2021).

[3] WMAP-Content of the Universe, [https://wmap.gsfc.nasa.gov/universe/uni\\_matter.html](https://wmap.gsfc.nasa.gov/universe/uni_matter.html)

[4] S. Navas et al. (Particle Data Group), Phys. Rev. D 110, 030001 (2024) Neutrino Masses, Mixing, and Oscillations

[5] The KATRIN Collaboration, *Direct neutrino-mass measurement with sub-electronvolt sensitivity*, Nature Physics, Volume 18, February 2022, 160–166.

[6] Garv Chauhanm R. Andrew Gustafson, Ian M. Shoemaker, *Supernova Gamma-Ray Constraints from Heavy Sterile Neutrino Decays* (arXiv:2503.13607v1 17 Mar 2025).

[7] GRAMS Collaborators, <https://github.com/wgseligman/GrampsSim>

[8] Geant4 Documentation, <https://geant4.web.cern.ch/docs/>

[9] NASA, U.S. Standard Atmosphere 1976

[10] LUX Collaboration, *Discrimination of electronic recoils from nuclear recoils in two-phase xenon time projection chambers* (Physical Review D 102, 112002 (2020))

[11] EXPACS Homepage in English, <https://phits.jaea.go.jp/expacs/index.html>

[12] The Astropy Project, <https://www.astropy.org>

[13] Arthur H. Compton, *X-rays as a branch of optics* (Nobel Lecture, December 12th, 1927)

## APPENDIX

### A: Compton Energy Reconstruction

For an event with two scatters and a third scatter/photo-absorption, the total energy of the primary gamma ray can be calculated as follows.  $E$  is the total energy of the primary gamma ray,  $E_1, E_2$  are the energy deposits in the first and second scatters,  $E'_3$  is the energy of the photon after the second scatter, and  $\theta'$  is the Compton angle of the second scatter.

$$E = E_1 + E_2 + E'_3,$$

$$E'_3 = -\frac{E_2}{2} + \sqrt{\frac{E_2^2}{4} + \frac{E_2 m_e c^2}{1 - \cos \theta'}}$$

Note that  $\theta'$  can be calculated using the three-dimensional position reconstruction capabilities of the LArTPC.

Uncertainty beyond ionization charge and position resolution arises from Doppler broadening. This is a spreading of the energy distribution as a result of Compton electrons not being at rest with respect to the atom. This phenomenon is more pronounced at lower energies,

so for the 30-100 MeV range considered for sterile neutrino signal it is not significant.

### B: Horizon Line Calculation

When considering the background flux from the cosmic diffuse emission, we want to take into account that the Earth itself can block a large fraction of the flux. To calculate how much, we estimate the Earth to be a perfect sphere and calculate at what angle from zenith the horizon line is.

Let  $R_e$  be the radius of the Earth and  $h$  be the height above Earth's surface (Figure 10). The line of view to the horizon will be tangent to the surface of the Earth, and thus will make a right angle with  $R_e$ . Then,

$$\alpha = \cos^{-1} \frac{R_e}{R_e + h}$$

$$\theta = 90^\circ + \frac{\alpha}{2}$$

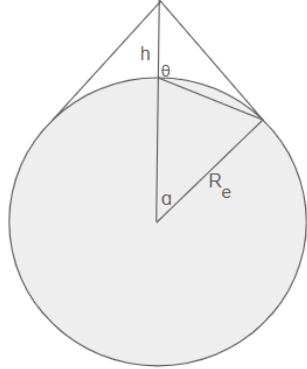


Figure 11. Geometric cross section of Earth.  $\theta$  is the angular below zenith that it is possible to view cosmic photons. This model does not account for refraction in Earth's atmosphere. However, gamma ray refractive indexes are incredibly small and can be taken to be negligible compared to the angular resolution of the detector.